

Failure Analysis of Electronic and Microelectronic Components with a New Automatic Target Preparation System

**Katja Reiter, Fraunhofer Institute for
Silicon Technology, Itzehoe, Germany**

Hans Bundgaard, Struers A/S, Denmark

STR UCT URE

**Struers  Journal
of Materialography
10/2006**

 **Struers**

Readers are invited to send in written contributions on the preparation of metallographic, mineralogical and ceramic specimens or related subjects.

Articles found suitable will be published free of charge in Structure with any accompanying illustrations in black and white or colour.

Articles should be sent to the editorial board of Structure as paper copy or electronically. If an article is supplied in electronic form, text and images should be saved in separate files.

The following formats are preferred:

Text: MS Word

Images: TIF or JPG in high resolution

Drawings: Corel Draw (CDR 10 or earlier)

or Adobe Illustrator (CS 11.0 or earlier)



Failure Analysis of Electronic and Microelectronic Components with a New Automatic Target Preparation System

Katja Reiter, Fraunhofer Institute for Silicon Technology, Itzehoe, Germany, katja.reiter@isit.fraunhofer.de

*Hans Bundgaard, Struers A/S, Ballerup, Denmark
hans.bundgaard@struers.dk*

1. Introduction

Electronic and microelectronic assemblies are complex material composites. The materials used are quite different in their chemical composition, their crystallographic structure and their microstructure. Of technical importance for the qualification of the components are interfaces, grain boundaries and phase boundaries as well as heterogeneous precipitations. Imaging and analysis of the microstructure is a prerequisite to estimate the quality of an assembly. Further criteria of qualification, from a metallographic point of view, are inclusions, contaminations, voids, cracks, holes, as well as the evaluation of contours, e.g. the wetting angle of a soft solder connection. [1]

In order to reach an excellent specimen surface, the samples have been prepared by hand up to the present day. So far only very experienced technicians have been able to work on difficult tasks such as thin wire bonds within intelligent chip modules. Another possibility is semi-automatic target preparation. The problem of both methods is that the specimen is in danger to be ground beyond the target layer and thus to be lost irretrievably, especially aiming at microscopic interior structures within complex electronic modules.

Based on the requirements regarding target, reproducibility, and specimen surface quality, an automatic system for controlled material removal and target preparation has been developed. The tool is for the metallographic failure analysis for electronics, and provides an accuracy of 5 μm . Fraunhofer ISiT has been able to obtain good results by running target preparation processes on the machine and has developed corresponding preparation methods.

2. Description of the Device

For automatically controlled material removal and preparation, the new tool offers alignment and measuring of the sample pri-



or to the preparation. Cross sections of mounted and unmounted samples can be ground and polished to visible and hidden targets. A laser measuring system assures an accuracy of $\pm 5 \mu\text{m}$ and the removal rate is automatically calculated during the preparation process.

Alignment and measuring can either be video based by a microscope for samples with a visible target (Fig. 1), or X-ray based for samples with a hidden target (Fig. 2).

The new tool then calculates the total amount of material to be removed, starts preparation, and automatically stops the plane grinding step at a fixed distance from the final target plane of $175 \mu\text{m}$.

At this point, a high precision measuring system takes control, and the following steps will take the preparation towards the target with breaks, as shown in Fig. 3, of preset, user-definable positions, e.g. $50 \mu\text{m}$ and $10 \mu\text{m}$.

The new tool automatically controls material removal by two separate measuring systems. Removal during grinding steps is controlled by an electronic measuring system, which continuously measures the distance to target.

In this fashion, the major part of the target distance is covered as quickly as possible. $175 \mu\text{m}$ from the target, a laser measuring system takes over. The system uses a relative measuring technique (Fig. 3). To achieve reliable measuring, the specimen is cleaned in two internal cleaning stations before moving to the laser measuring station. The use of laser measuring gives the system an accuracy of $\pm 5 \mu\text{m}$ (Fig. 4). [2]

3. Preparation Method

Before starting the preparation, the is fixed with a special adhesive to a cross section jig, *sample chair*. The sample chair is then clamped into the sample holder and aligned and measured with X-ray in real time (Fig. 5).

Measured data is transmitted to the preparation system, and the sample holder positioned in the sample mover of the polishing machine. Before preparation starts, the sample height is measured and the removal time calculated for each of the steps. Table 1 describes the process summary and the polishing method of six samples with $20 \mu\text{m}$ gold wire bonds.

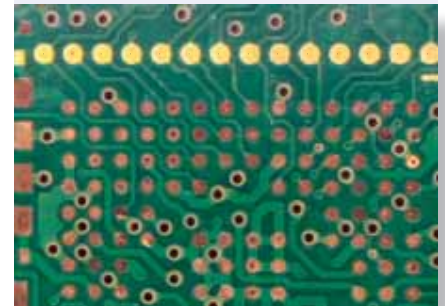


Fig. 1: Printed Circuit Board with visible target, a row of microvias

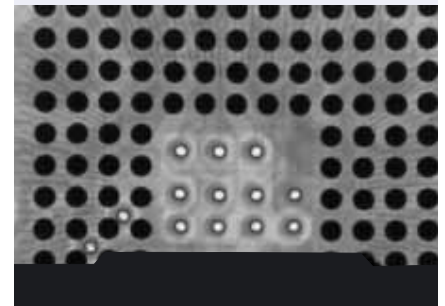


Fig. 2: Radiographic image of hidden target, a row of solder balls on a CSP-component

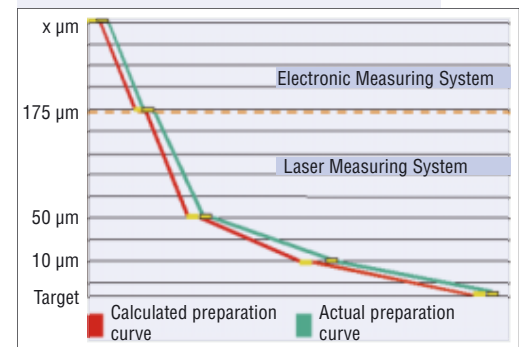


Fig. 3: Electronic and Laser measuring systems

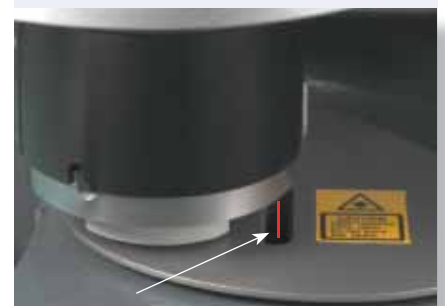


Fig. 4: Laser measuring system

Sample	1	2	3	4	5	6
Polishing/Grinding media	Removal [μm]	Removal [μm]	Removal [μm]	Removal [μm]	Removal [μm]	Removal [μm]
SiC#800	1691	1653	1697	1622	1677	1682
SiC#1200	261	260	256	254	253	255
MD-Sat 9 μm	19	15	12	28	26	22
MD-Dur 3 μm	2 min	2 min	2 min	2 min	2 min	2 min
OP-Chem 0.25 μm	0.5 min	0.5 min	0.5 min	0.5 min	0.5 min	0.5 min
Target value	1971	1926	1965	1898	1958	1961
Distance to target	2	-2	0	-4	2	2
Time	34 min	34 min	35 min	36 min	31 min	32 min

Table 1: Process summary of wire bond preparation.

The polishing process is interrupted according to predefined polishing times in order to allow a periodical laser measurement of the sample. The laser measurement allows an exact observation and control of the alignment to ensure that the targets will be reached exactly as intended. The automatic preparation permits high precision as shown in Fig. 5-8. The 20 μm bonding wire is visible along the complete length (Fig. 6) and also a crack on the wedge side is documented (Fig. 8).

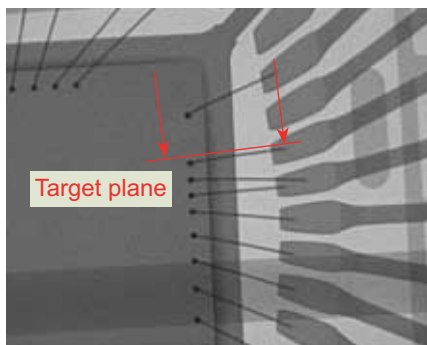


Fig. 5: Real-time target alignment and measuring using x-ray and special set-up station

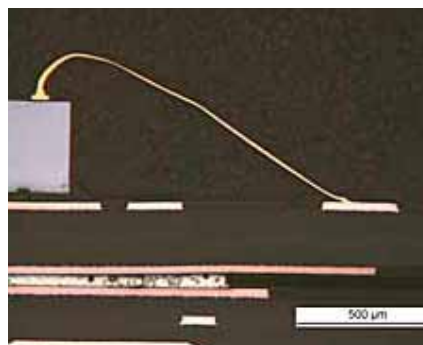


Fig. 6: The entire length of the 20μm gold wire is visible in the cross section

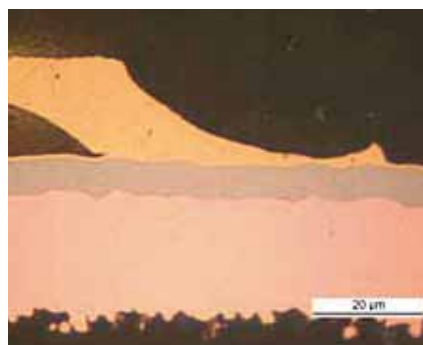


Fig. 7: Wedge side of the wire

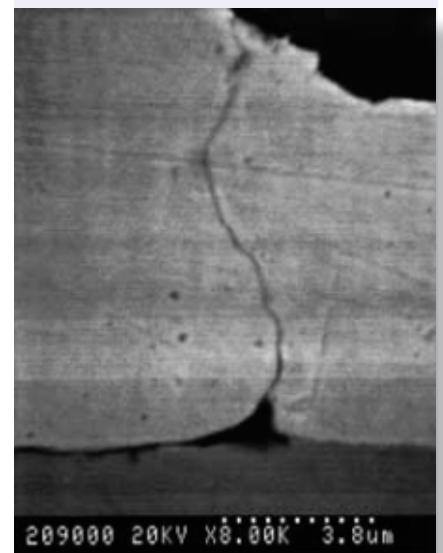


Fig. 8: SEM image of wedge bond with crack

4. Evaluation of the Device

The target surface quality depends on various factors:

- Grinding/polishing media
- Polishing time and force
- Mounting

It is essential to apply the correct pressure force and to choose the right polishing cloths and suspensions. It is recommended to use the diamond suspensions which exactly match the polishing cloths. The set removal time results from the depth of deformation, caused by the grinding or polishing media.

For instance, in Step 2 (grinding with silicon carbide paper) it is recommended to preset the total removal at 250 μm . Table 2 shows the optimized preparation parameters.



Step	1	2	3	4	5
Surface	MD-Fuga	MD-Fuga	MD-Sat	MD-Dur	MD-Chem
Abrasive	SiC	SiC	Diamond	Diamond	OP-S
Grit/grain size	800	1200	9 μm	3 μm	0.25 μm
Lubricant	Water	Water			
RPM	300/150	300/150	300/150	150/150	150/150
Force	30 N	30 N	25 N	15 N	15 N
Time	Dependant on the sample material and its grinding behavior			2 min	0.5 min
Removal	Target	250 μm	20 μm		

Table 2: Optimized preparation parameters

It is also essential to choose the correct mounting material.

For filigree structures, such as microvias in printed circuit boards or thin wire bonds, epoxy resins fill and adhere better to cracks and holes. The preparation results achieved are in line with the specifications of the tool manufacturer, i.e. the required precision of $\pm 5\mu\text{m}$ will indeed be achieved. However to get such exact results it is essential to work accurately.

The following factors can cause deviation in target measurement:

- Wet sample and/or reference plane by laser measuring after cleaning process
- Person doing the initial measurement did not work accurately



5. Examples of preparation

The evaluation of electronic devices (quality of production and reliability) offers a number of samples for the metallographic target preparation system. The following images show typical objects of examination in the analysis of microstructures and materials in the electronics packaging industry with brief comments.

Underfilling CSP

Underfill is typically used only to encapsulate flip chip components at the board level. However, the application for fine-pitch BGAs and CSPs in handheld devices, such as cell phones and PDAs, in automotive electronics, and in military applications, is increasing as the need for greater miniaturization and higher performance grows. In these applications, mechanical stresses can induce early failures.

Fig. 9 -16 show examples of solder joint evaluation of under-filled CSPs after different loads (e.g. thermal shock cycles of $-40/+125^{\circ}\text{C}$, humidity and ultrasonic testing).

The underfilled area component is an example of a preparation of a hidden target.

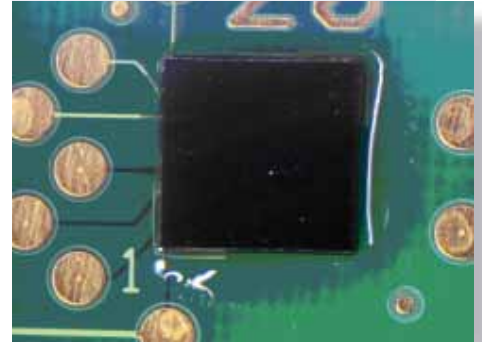


Fig. 9: Overview (optical inspection) of underfilled CSP

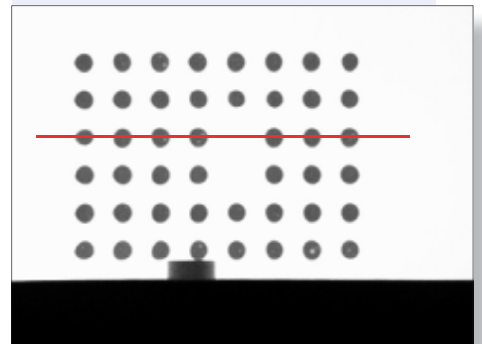


Fig. 10: Radiographic image of CSP mounted in sample holder

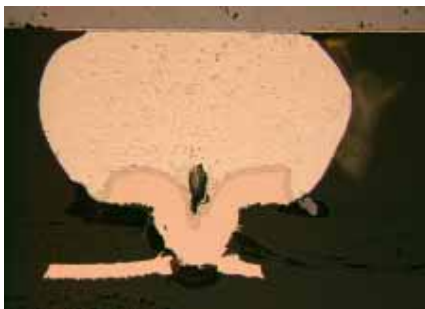


Fig. 11: Microsection of SnAgCu 0.5-CSP ball with damaged copper trace after thermal cycling (1000x)

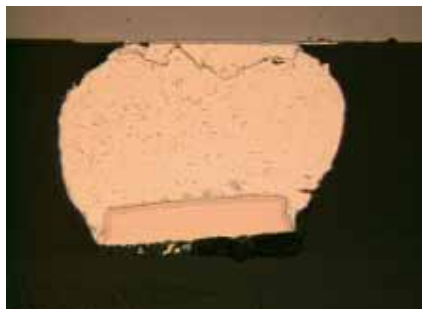


Fig. 12: Cu-pad lift off from PCB and solder crack after thermal cycling (1500x)

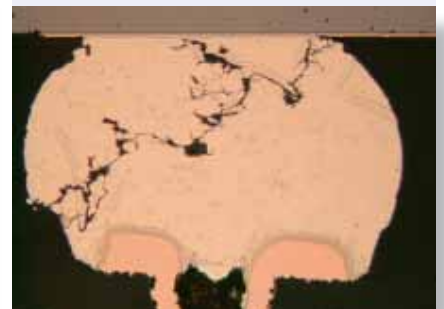


Fig. 13: Microvia: lift-off from PCB and solder crack after thermal cycling (1500x)

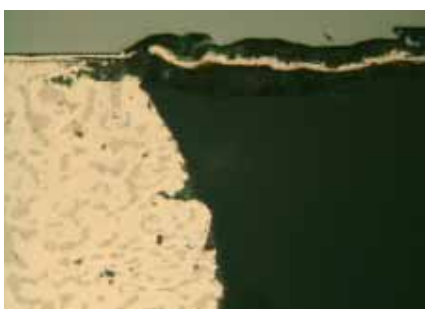


Fig. 14: Gap between underfill and Silicon-chip after ultrasonic testing



Fig. 15: Brittle fracture after thermal cycling (1500x)

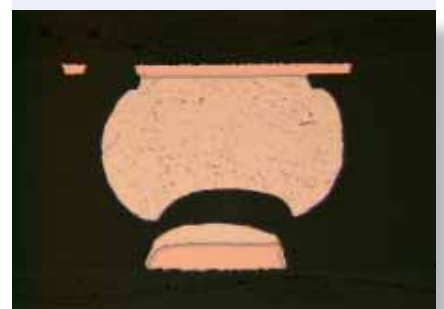


Fig. 16: Cold soldering and lift-off after thermal cycling (1500x)

Some lead free phenomena's

The European Union has set in place a Restriction of Hazardous Substances (RoHS) directive that states: "Member States shall ensure that from July 1, 2006, new electronic equipment put on the market does not contain lead (Pb), mercury, cadmium, hexavalent chromium, polybrominated biphenyls and polybrominated diphenyl." With the use of lead free alloys (e.g. SnAgCu – SAC) new effects and challenges will occur. The preparation method shown in Table 2 was developed for lead free alloys. Its functionality is demonstrated below.

Leaching

Dissolution is necessary for forming the initial intermetallic compounds in solder joints. Dissolution is the metallurgical change that takes place as solid materials melt into liquid materials. Leaching of metal substrates and their protective metal coatings occurs during soldering operations including wave soldering operations, reflow, rework, and repair.

Precious metal surface finishes (i.e. silver, gold, and palladium) and base substrates (copper and nickel) are involved in the dissolution process. The rate of dissolution depends upon the composition of the base metal and solder, cleanliness, and solders velocity. The dissolution rate also varies exponentially with temperature [3].

The sample (Fig. 17-19) shows a thin braided wire with 7 cores dipped in molten lead free solder three times at 260°C. Fig. 17 shows the state before dipping; and Fig. 18 shows the strong dissolution of the copper wire in SnAgCu 0.5 solder. There is only one core left. The other six cores are dissolved.

Cause for this strong dissolution is the low copper content inside the solder alloy. With the saturation of copper in the solder alloy (use of SnAgCu 1.3, Fig. 19) the dissolution will be reduced significantly. For the usage of a lead free solder alloy this fact should be noted.

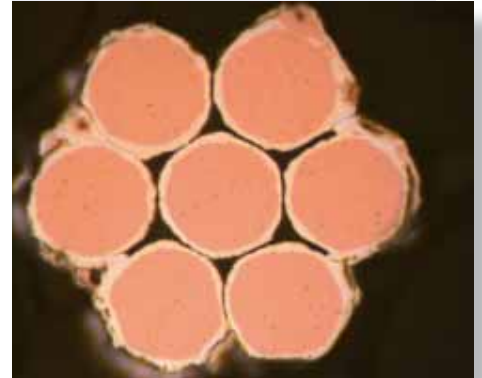


Fig. 17: Status quo of the braided wire before dipping (1000x, micro section)

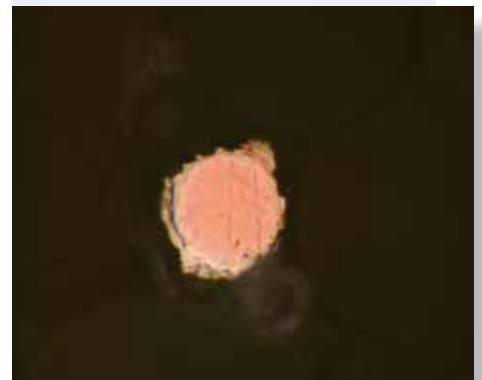


Fig. 18: SnAgCu 0.5 – strong dissolution (1000x)



Fig. 19: SnAgCu 1.3 – lower dissolution rate because of copper saturation in solder alloy (1000x)

Whisker growth

Tin whiskers are growth structures of small diameter ($\sim 1 \mu\text{m}$) that develop out of pure tin plated surfaces. The growth can cause short circuits or functional damage to another part of the product. [4]

With the accuracy of the tested preparation method it was possible to display single whiskers in the microsection (see Fig.s 20-23).

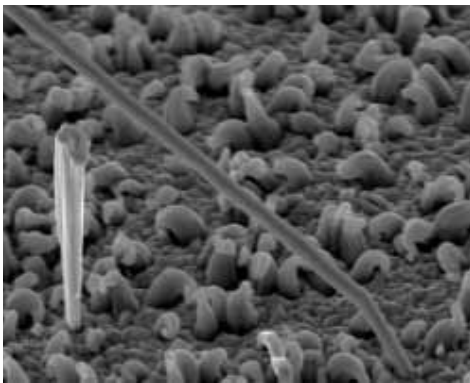


Fig. 20: SEM image of a galvanic pure tin surface with different shapes of whiskers



Fig. 21: Microsection of tin layer with grown whisker (preparation plane measured with optical measuring station)

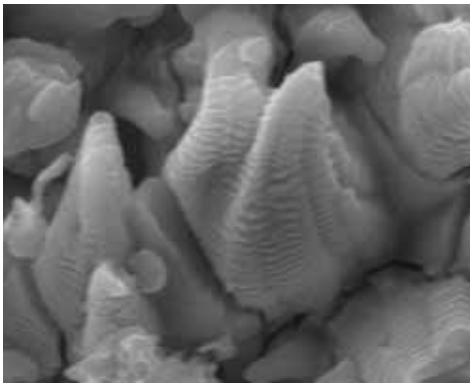


Fig. 22: SEM image of jelly cap whisker (5000x)



Fig. 23: Microsection of jelly cap whisker (1000x)

Tin whiskers can form in a wide range of shapes, length and sizes.

Two different whisker shapes are shown in the pictures (needles – Fig. 20-21; and jelly caps - Fig. 22-23). Whisker growth is attributed to the driving force to relieve internal stress that is created during the coating process, and during bending, forming and similar mechanical actions on tin plated structures.

Brittle fracture

The electroless nickel immersion gold (ENIG) surface is a possible replacement for the lead containing printed circuit board surface (normally hot air solder leveling). However, a brittle fracture problem seen with ENIG surface causes premature solder joint failures and low shear forces after assembly.[5]

Few solder joints are weaker than the surrounding normal joints, making it difficult to test for, find, and eliminate the phenomenon. The brittle fracture failure mode is limited to assemblies with a surface finish of immersion gold / electroless nickel. It is caused by a corrosion mechanism that occurs during the auto-catalytic immersion gold process. The gold deposition selectively attacks grain boundaries in the phosphorous enriched nickel layer, causing mud-flat cracks in the electroless nickel layer.

The typical failure mode of this phenomenon is the separation between the nickel layer and the intermetallic phase.
(Fig. 24-26)

Fig. 26 shows a relatively thick intermetallic phase which is unusual for the system of SnNi. Normally the intermetallic phase is thinner than $1\ \mu\text{m}$. The thick intermetallic phase ($2\text{-}3\ \mu\text{m}$) is an indicator for brittle fracture. Another indicator is the enrichment of phosphorous in the interface boundary of the nickel intermetallic phase.

6. Conclusions

The new automatic preparation system evaluated in this work can be used for the metallographic failure analysis on electric and microelectronic components.

The desired preparation layers were achieved precisely and reproducibly with several specimens of the same kind. By hand, only experienced and skilled technicians can prepare such specimens of good quality, and still it is difficult and time consuming. Typically the specimens are at risk of being ground beyond the target and lost for further investigations.

The automatic preparation system, however, allows the preparation of critical samples within a short time, with high precision and with an excellent reproducibility.

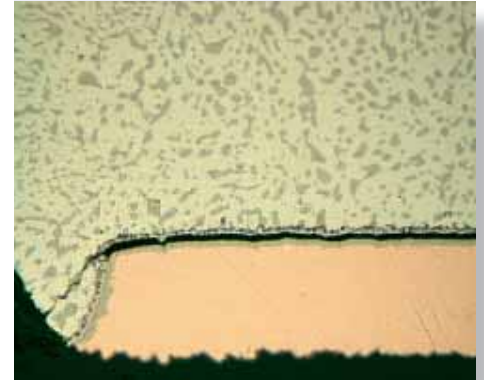


Fig. 24: Microsection (overview) with the brittle fracture between intermetallic phase and Nickel layer (200x)

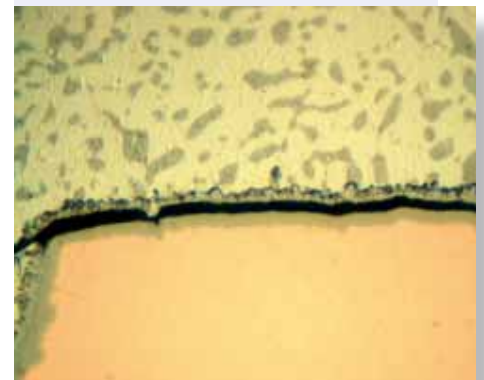


Fig. 25: Brittle fracture between intermetallic phase and Nickel layer (detail 500x)

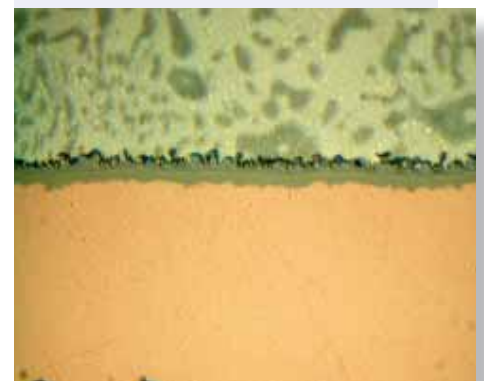


Fig. 26: Thick SnNi intermetallic phase as indication for increased risk of brittle fracture (1000x)

7 References

- [1] Structure 34: Special aspects of the metallographic preparation of electronic and microelectronic devices, K. Reiter, M. Reiter, Dr. T. Ahrens, Fraunhofer Institute for Silicon Technology, Itzehoe, Germany
- [2] Struers Application Notes:
“Metallographic preparation of Microelectronics”, Elisabeth Weidmann, Anne Guesnier, Hans Bundgaard, Struers A/S, Copenhagen, Denmark Internet: www.struers.com
- [3] R.J. Klein Wassink, “Soldering in Electronics” 1991
- [4] Dr. Hans Bell “Reflowlöten: Grundlagen, Temperaturprofile und Lötfehler” 2005
- [5] Sven Lamprecht, Dr. H.-J. Schreier
“Impacts of the bulk Phosphorous content of electroless Nickel layers to Solder Joint Integrity and the use as Au/Al- wire bond surface” Atotech Germany GmbH 2004